

# *peri*-Xanthenoxanthene (PXX): a Versatile Organic Photocatalyst in Organic Synthesis

Cristofer Pezzetta,<sup>a, b</sup> Andrea Folli,<sup>a</sup> Oliwia Matuszewska,<sup>a</sup> Damien Murphy,<sup>a</sup> Robert W. M. Davidson,<sup>b,\*</sup> and Davide Bonifazi<sup>a, c,\*</sup>

<sup>a</sup> School of Chemistry, Cardiff University,  
Park Place, Cardiff CF10 3AT United Kingdom

<sup>b</sup> Dr. Reddy's Laboratories (EU),  
410 Science Park, Milton Road, Cambridge,  
CB4 0PE, United Kingdom  
Phone: +44 1223651443  
E-mail: rdavidson@drreddys.com

<sup>c</sup> Institute of Organic Chemistry, Faculty of Chemistry,  
University of Vienna, Währinger Strasse 38,  
1090, Vienna, Austria  
Phone: +43-1-4277-52158  
E-mail: davide.bonifazi@univie.ac.at

Manuscript received: January 26, 2021; Revised manuscript received: March 12, 2021;  
Version of record online: ■■, ■■■



Supporting information for this article is available on the WWW under <https://doi.org/10.1002/adsc.202100030>

© 2021 The Authors. *Advanced Synthesis & Catalysis* published by Wiley-VCH GmbH. This is an open access article under the terms of the Creative Commons Attribution Non-Commercial NoDerivs License, which permits use and distribution in any medium, provided the original work is properly cited, the use is non-commercial and no modifications or adaptations are made.

**Abstract:** Recent years have witnessed a continuous development of photocatalysts to satisfy the growing demand of photophysical and redox properties in photoredox catalysis, with complex structures or alternative strategies devised to access highly reducing or oxidising systems. We report herein the use of *peri*-xanthenoxanthene (PXX), a simple and inexpensive dye, as an efficient photocatalyst. Its highly reducing excited state allows activation of a wide range of substrates, thus triggering useful radical reactions. Benchmark transformations such as the addition of organic radicals, generated by photoreduction of organic halides, to radical traps are initially demonstrated. More complex dual catalytic manifolds are also shown to be accessible: the  $\beta$ -arylation of cyclic ketones is successful when using a secondary amine as organocatalyst, while cross-coupling reactions of aryl halides with amines and thiols are obtained when using a Ni co-catalyst. Application to the efficient two-step synthesis of the expensive fluoro-tetrahydro-1*H*-pyrido[4,3-*b*]indole, a crucial synthetic intermediate for the investigational drug setipiprant, has been also demonstrated.

**Keywords:** PXX; xanthenoxanthene; photocatalysis; C–C; C–S; C–N;  $\beta$  arylation; mechanism; EPR; photoredox; highly reducing photocatalyst

## Introduction

The field of photoredox catalysis has seen a huge increase in popularity in the last decade, with numerous useful transformation being discovered that were not possible, or were much more difficult to obtain, with non-photoredox methods.<sup>[1]</sup> The ability to generate reactive radical species in very mild conditions is

surely at the root of this popularity. Ru(II)- and Ir(III)-based complexes are the work-horses in the field: chemical stability, long excited state lifetimes and tunability of the photoredox properties through ligand modifications are among the reasons for this preference in the community.<sup>[1b]</sup> Early works revealed that *fac*-[Ir(ppy)<sub>3</sub>], a homoleptic complex of Ir(III) (Figure 1), was particularly interesting for the strong

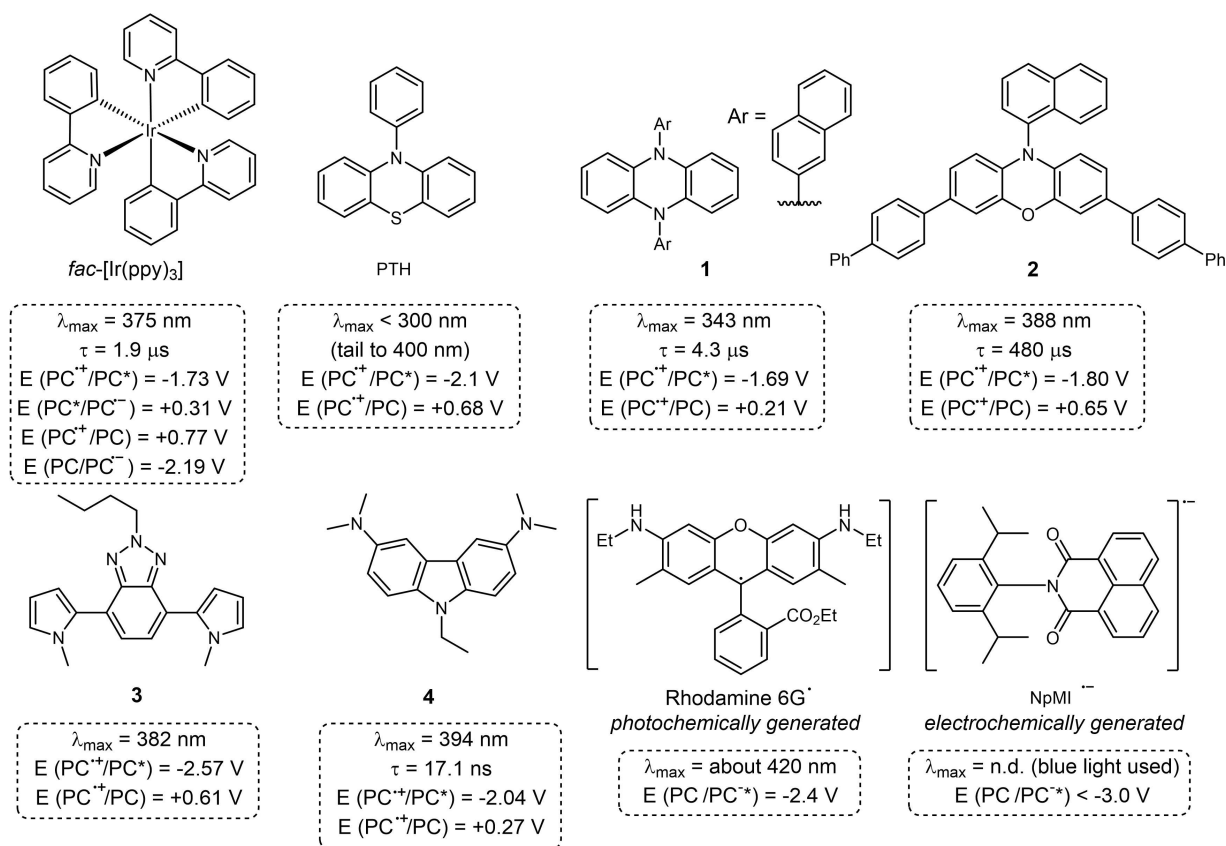


**Figure 1.** Selection of highly reducing photocatalysts and photocatalytic systems from the literature, along with their reported photophysical properties. Reduction potentials reported vs SCE in  $\text{CH}_3\text{CN}$ .<sup>[1b,4a,5a,6,7,8b,f]</sup>

reductive properties of its excited state.<sup>[2]</sup> With a redox potential of  $-1.73$  V vs SCE, it can be used effectively for the activation of alkyl and aryl halides to form organic radical intermediates.<sup>[2b-d]</sup> The peculiar reactivity found with *fac*-[Ir(ppy)<sub>3</sub>] inspired further work towards the search of alternative photocatalytic systems with comparable or higher reducing power (Figure 1), especially to trigger photoredox activation of non-accessible substrates because of their lower reduction potentials. The interest focused mainly on the development of organic dyes, so that reaction mixtures could be devoid of metallic impurities, and to avoid the use of expensive and supply-dependent precious metals.<sup>[1c,f]</sup> The reduction of organic halides has typically been used as a benchmark reaction, either for dehalogenation and formation of the corresponding hydrocarbon, or for addition to electron-rich radical traps (benzene, pyrrole and similar).<sup>[3]</sup> This is the case of phenothiazine (PTH)-based photocatalysts,<sup>[4]</sup> whose use was also recently demonstrated for the activation of *in situ*-formed arylsulfonium ions.<sup>[4c]</sup> Similarly, dihydrophenazine **1** and phenoxazine **2** were exploited for the synthesis of  $\text{CF}_3$ -bearing heterocycles, and as photocatalysts for C–N and C–S bond-forming cross-coupling reactions as well.<sup>[5]</sup> Benzotriazole **3** was

designed for the activation of aryl iodides and subsequent radical addition to furans.<sup>[6]</sup> Carbazole **4** showed a very low reduction potential, allowing activation of aryl chlorides and fluorides alike.<sup>[7]</sup> A different strategy involved the photoexcitation of an electron-rich transient species, being it an anion, a photocatalytically-formed radical anion, an electrochemically-formed radical anion, a neutral radical or an excited state.<sup>[8]</sup> In these cases the excited state of the transient species is extremely electron-rich, often capable of reducing electron-rich aryl halides to their corresponding aryl radicals.<sup>[8f,g,i]</sup> Two-photon excitation of a water soluble *fac*-Ir(ppy)<sub>3</sub> analogue also allowed the formation and synthetic utilisation of highly reducing hydrated electrons.<sup>[8j]</sup> Other strategies involved the sensitisation of pyrene with [Ru(bpy)<sub>3</sub>]<sup>2+</sup> as visible light photocatalyst,<sup>[9]</sup> and triplet-triplet annihilation for the generation of a high-energy singlet excited state.<sup>[10]</sup> In most of the aforementioned cases, demonstrations of photocatalytic activity have been restricted to a few benchmark reactions (dehalogenation, addition to radical traps) and limited efforts have been dedicated to expand the chemical space of their reactivity.<sup>[4c,5]</sup>

Considering all the efforts gone to the development of highly reducing organic photocatalysts, it is surprising that a molecule as simple as PXX (*peri-xanthenoxanthene*, Figure 2a), the *O*-doped analogue of anthanthrene, has been so far disregarded. Structural simplicity, ease of synthesis (see SI) and low cost (raw material cost estimated at £2.30/mmol, see SI) would make it an appealing alternative to the more expensive and structurally complex photocatalysts previously mentioned.

The use of PXX is inherited from organic semiconductor chemistry, as substituted PXX derivatives show excellent carrier-transport and electron injection properties, easy processability, chemical inertness and exceptional thermal stability.<sup>[11]</sup> This made them a good choice for applications as organic semiconductors in transistors,<sup>[12]</sup> as conducting polymers<sup>[13]</sup> or prepar-

ing p-type graphenoid structures.<sup>[11,14]</sup> PXX itself is a bright yellow solid, showing absorption in the UV and visible spectrum, with a lower energy peak at 439 nm (blue light) in CH<sub>3</sub>CN (Figure 2b,c).<sup>[14a]</sup> Besides visible light absorption, of uttermost interest are the electrochemical properties of both PXX ground state and singlet excited state (Figure 2c). In the S<sub>1</sub> state (PXX\*), a remarkable reduction potential  $E^{1/2}(\text{PXX}^{\bullet+}/\text{PXX}^*)$  of  $-2.00$  V vs SCE has been calculated, suggesting the possibility of an efficient SET reduction of a number of organic substrates (Figure 3). The resulting PXX radical cation has a discrete potential (+0.77 V), allowing turnover of the photocatalytic cycle through oxidation of electron-rich reagents. In an effort to probe the photocatalytic properties of PXX, our group showed that the dehalogenation of a set of electron-poor aryl and alkyl halides could be achieved

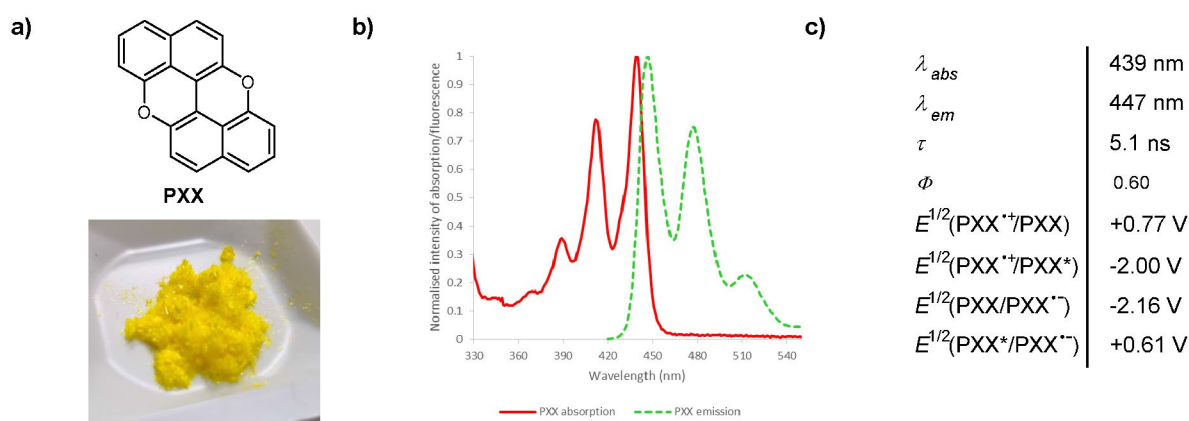


**Figure 2.** Properties of PXX: (a) structure and appearance; (b) absorption and emission ( $\lambda_{exc}$  at 412 nm) spectra of a  $10^{-4}$  M solution in CH<sub>3</sub>CN; (c) summary of photophysical and electrochemical properties.<sup>[14a]</sup> Photophysical data determined in CH<sub>3</sub>CN, electrochemical data determined vs SCE in CH<sub>3</sub>CN.

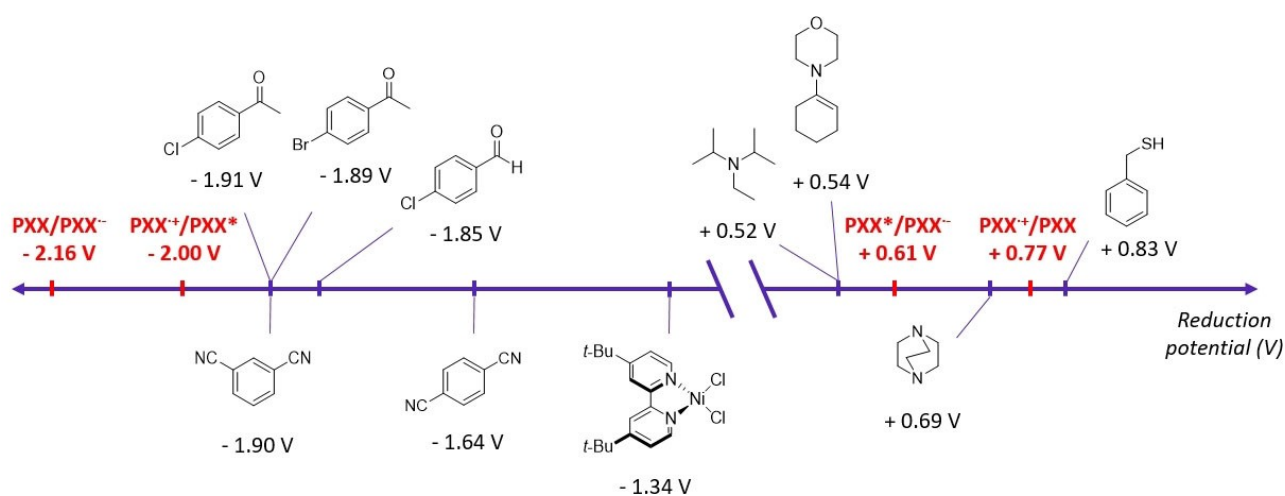


**Figure 3.** Reduction potentials of selected organic compounds compared to ground and excited state reduction potentials of PXX. Values given vs SCE in CH<sub>3</sub>CN.<sup>[15,16]</sup>

upon irradiation with blue light (450 nm) in the presence of DIPEA as electron donor.<sup>[14a]</sup> These preliminary investigations prompted us to further investigate the potentiality of PXX as a more general, highly reducing photocatalyst, capable of promoting a variety of different transformations.<sup>[17]</sup> The possibility to employ dual-catalytic platforms, wherein PXX photocatalysis could be coupled to another catalytic system, was also considered in our investigations.

Herein, we demonstrate the use of PXX as photocatalyst for the formation of C–C bonds *via* activation of organic halides and subsequent reaction with radical traps. The  $\beta$ -arylation of cyclic ketones is also shown when a secondary amine is introduced as organocatalyst. The formation of C–N and C–S bonds when coupled with nickel catalysis is also tackled, and the application to a synthetic intermediate of setipiprant through preparation of the corresponding *N*-aryl hydrazine precursor demonstrated. The mechanism of the transformations were further studied by photo-physical and EPR studies to confirm the role of PXX as photoreducing catalyst.

## Results and Discussion

### Activation of Organic (Pseudo)halides and Addition to Radical Traps

Our investigations started with an attempt to extend the observed activation of aryl halides to the formation of C–C bonds. Radical traps such as benzene and *N*-methylpyrrole were introduced to reaction mixtures containing the given aryl halide, PXX and a base. The arylation of benzene with 4'-bromoacetophenone was obtained when benzene was used as solvent in the presence of DBU as base (Table 1, see SI for more details). The reaction afforded a 42% yield when carried out at 50 °C (entry 1), while a reduced 19% yield was obtained at 25 °C (entry 2). Extended

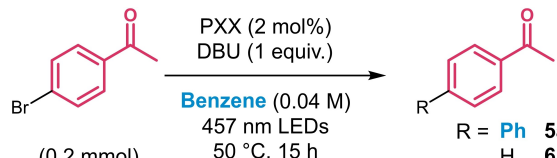
reaction times allow improvement in yields only when an additional loading of PXX is added (entries 3–4), suggesting degradation of the photocatalyst during the reaction.

The arylation of *N*-methylpyrrole proved more successful: two sets of conditions were found to be productive (Scheme 1). Method A involved the use of Cs<sub>2</sub>CO<sub>3</sub> as base in CH<sub>3</sub>CN at 50 °C (see SI for more details), and allowed the efficient arylation of 4'-bromoacetophenone and 4-bromobenzaldehyde in 71% and 75% isolated yields, respectively (**5b** and **5c**). These conditions performed poorly with other aryl halide substrates. However, when carrying out the reaction in DMSO with DIPEA as base at 25 °C (Method B),<sup>[9]</sup> a number of aryl bromide and chloride derivatives could be reacted, including those bearing ester (**5d**) and nitrile (**5e**, **5h**) groups. The activation of bromopentafluorobenzene was also successful, and compound **5f** obtained in 61% yield in a 2.4:1 isomeric ratio.<sup>[18]</sup> Heterocyclic bromides were not amenable of efficient activation, with compounds **5g** and **5i** obtained in limited yields. Other radical traps were also tested: while thiophene did not provide **5j** in useful yields, 1,3,5-trimethoxybenzene proved an efficient trap affording **5k** in 58% yield. The formation of C–Heteroatom bonds could be also probed, with the reaction with triethylphosphite affording **5l** in 66% yield.<sup>[19]</sup> The borylation with B<sub>2</sub>pin<sub>2</sub> gave **5m** in low yield (25%);<sup>[20]</sup> further attempts with modified conditions did not provide any significant improvements.

The activation of electron-poor alkyl halides is also feasible with PXX. For example, when diethyl 2-bromo-2-methylmalonate was reacted with indole in the presence of lutidine as base, the coupling product **5n** was obtained in 66% yield (Scheme 2a).<sup>[21]</sup> Analogously, MacMillan's arene trifluoromethylation<sup>[22]</sup> could be readily obtained (Scheme 2b) using triflyl chloride. In the reaction with *N*-methylpyrrole, both mono- and bis-trifluoromethylation were observed: **5o** in 33% yield and **5p** in 57% yield, respectively. With 3-methylbenzofuran, the main product was **5q** (59%, some was lost during purification due to the high volatility). Pleasingly, when the same conditions were applied to the perfluoroalkylation of 3-methylbenzofuran with perfluorohexyl iodide, an 82% yield of coupled product, **5r**, was obtained.

The mechanism of these transformations was subsequently examined. Electrochemical data and results from fluorescence quenching experiments are reported in Table 2. Building on the calculated reductive and oxidative properties of PXX\* ( $E^{1/2}(\text{PXX}^{\bullet+}/\text{PXX}^*) = -2.00 \text{ V vs SCE}$ ;  $E^{1/2}(\text{PXX}^*/\text{PXX}^{\bullet-}) = +0.61 \text{ V vs SCE}$ ),<sup>[14a]</sup> we conjectured that PXX\* is capable of photoreducing all the aryl halide substrates (Table 2) and at the same time to oxidise DIPEA ( $E^{1/2}_{\text{ox}} = +0.52 \text{ V vs SCE}$ , entry 5), but not *N*-methylpyrrole ( $E^{1/2}_{\text{ox}} = +1.04 \text{ V vs SCE}$ , entry 6). These

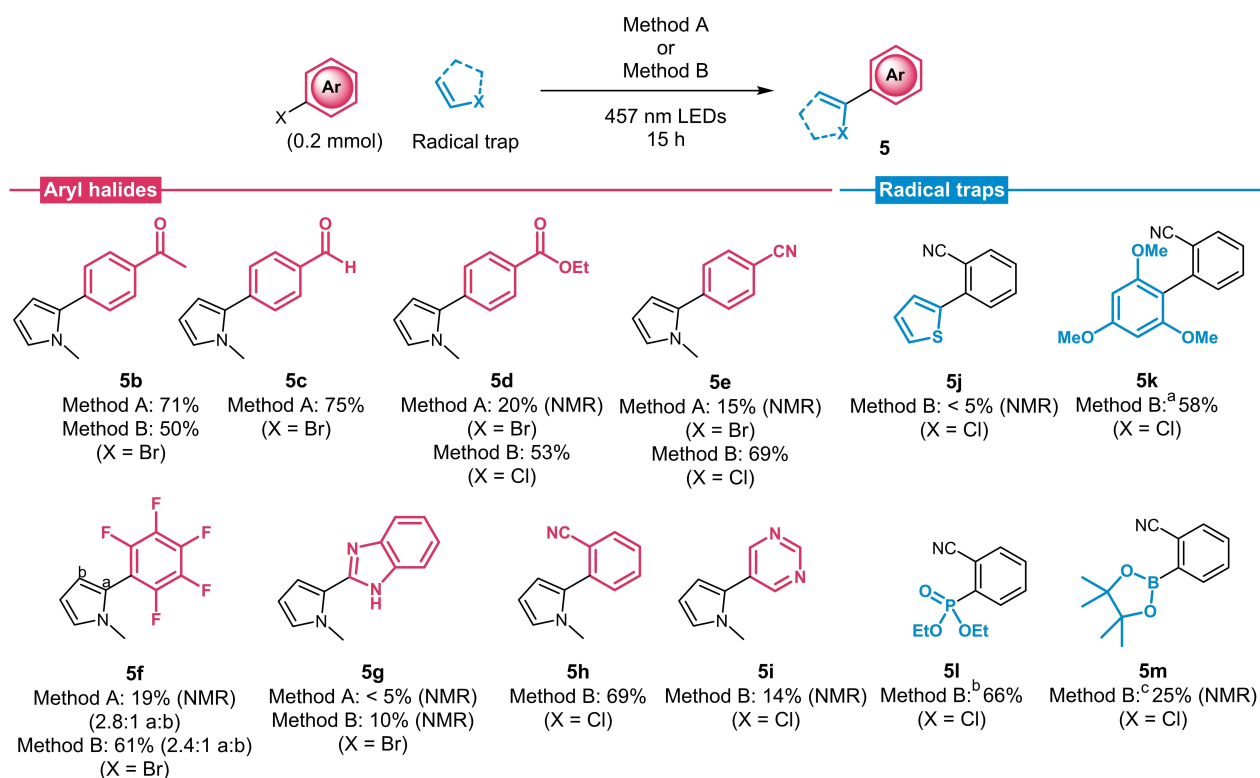
**Table 1.** The arylation of benzene with 4'-bromoacetophenone.



#	Modification	<b>5a</b> % <sup>[a]</sup>	Conv. % <sup>[a]</sup>	<b>6</b> % <sup>[a]</sup>
1	–	42	54	8
2	Run at 25 °C	19	26	< 5
3	Run for 40 h	40	60	17
4	Run for 64 h <sup>[b]</sup>	53	75	18

<sup>[a]</sup> Determined by <sup>1</sup>H-NMR analysis of reaction mixtures, using 1,3,5-trimethoxybenzene or CH<sub>3</sub>NO<sub>2</sub> as internal standard.

<sup>[b]</sup> Additional 2 mol% PXX added after 40 h.



**Scheme 1.** Scope of aryl halides and radical traps in the PXX-catalysed arylation reaction. Method A: radical trap (20 equiv.), PXX (2 mol%), Cs<sub>2</sub>CO<sub>3</sub> (1.2 equiv.), Acetonitrile 0.1 M, 50 °C. Method B: radical trap (10 equiv.), PXX (2 mol%), DIPEA (1.4 equiv.), DMSO 0.2 M, 25 °C. Isolated yields reported unless otherwise stated. Notes: <sup>[a]</sup> 20 equiv. of 1,3,5-trimethoxybenzene were used. <sup>[b]</sup> 5 equiv. of triethyl phosphite were used. <sup>[c]</sup> 3 equiv. of B<sub>2</sub>pin<sub>2</sub> were used, along with a DMSO:H<sub>2</sub>O 9:1 solvent system.

**Table 2.** Redox potentials and quenching studies on PXX (4 × 10<sup>-5</sup> M in CH<sub>3</sub>CN, intensity of fluorescence recorded at 477 nm).

#	Quencher	<i>E</i> <sub>red</sub> (V) <sup>[a]</sup>	<i>k</i> <sub>Q</sub> (M <sup>-1</sup> s <sup>-1</sup> ) <sup>[b]</sup>
1	4-Bromoacetophenone	-1.89 (r)	1.3 × 10 <sup>10</sup>
2	4-Bromobenzaldehyde	-1.76 (r)	1.8 × 10 <sup>10</sup>
3	2-Chlorobenzonitrile	-1.80 (r)	3.2 × 10 <sup>8</sup>
4	DIPEA	+0.52 (o)	3.5 × 10 <sup>7</sup>
5	<i>N</i> -Methylpyrrole	+1.04 (o)	N.D. <sup>[c]</sup>

<sup>[a]</sup> Determined in DMF (entry 3) or CH<sub>3</sub>CN (other entries) vs SCE; (r) refers to a reduction of the quencher, (o) to an oxidation of the quencher. Obtained from references<sup>[15]</sup> (entries 1–2, 4–5) and<sup>[24]</sup> (entry 3).

<sup>[b]</sup> Entries 1, 2, 4: obtained from reference<sup>[14a]</sup>. Entries 3, 5: calculated from Stern Volmer plots as *k*<sub>Q</sub> = *K*<sub>SV</sub>/τ<sub>0</sub> where τ<sub>0</sub> is the lifetime of PXX\* without quencher (5.1 ns in CH<sub>3</sub>CN).<sup>[14a]</sup>

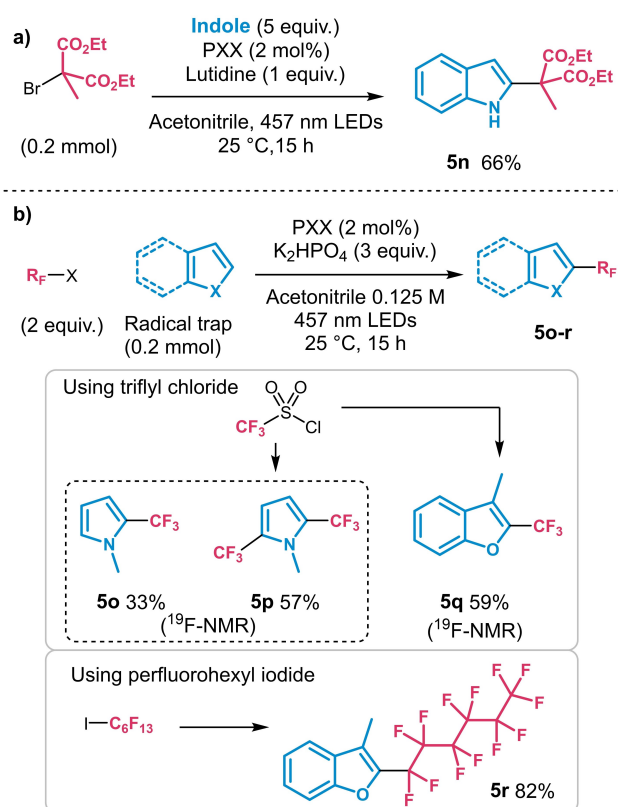
<sup>[c]</sup> No quenching observed.

considerations mirror Stern-Volmer investigations<sup>[23]</sup> which showed that the fluorescence quenching rates (*k*<sub>q</sub>, Table 2) observed for PXX with all aryl halides (from 10<sup>8</sup> to 10<sup>10</sup> M<sup>-1</sup> s<sup>-1</sup>, entries 1–3) are considerably higher than those determined in CH<sub>3</sub>CN with DIPEA

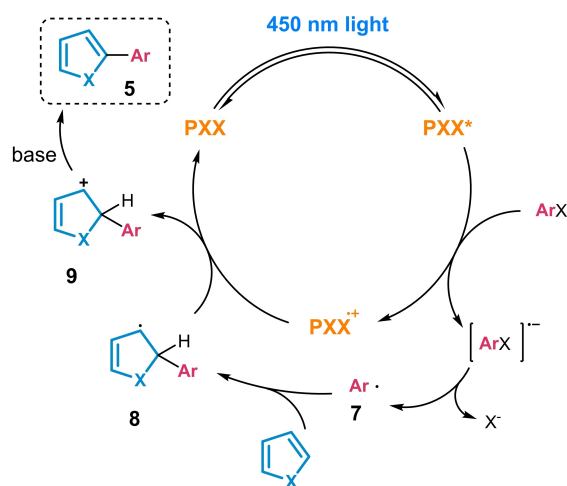
(3.5 × 10<sup>7</sup> M<sup>-1</sup> s<sup>-1</sup>, entry 4) and *N*-methylpyrrole, for which no quenching was observed (entry 5). This suggests that, under illumination, aryl radicals are formed together with PXX<sup>•+</sup>, as also reported in a previous work by us.<sup>[14a]</sup> Based on the information gathered, the most likely mechanistic pathway is outlined in Scheme 3.<sup>[3]</sup> After photoreduction of the aryl halide and formation of the corresponding aryl radical (7), this reacts with suitable unsaturated systems (radical traps) to form the new C–C bond. Oxidation of the resulting radical adduct 8 by PXX<sup>•+</sup> and subsequent deprotonation of 9 close the catalytic cycle.

### Merging Organo- and Photocatalysis: β-Arylation of Carbonyl Compounds

The merging of photoredox catalysis with organo-catalysis has been among one of the main initiators of the field, with the α-alkylation of aldehydes from Nicewicz and MacMillan being the seminal example.<sup>[25]</sup> Typical organocatalysis intermediates such as enamines and iminium ions can readily participate in redox and radical reactions, either in conjunction with a photocatalyst or by exploitation of their intrinsic photoreactivity.<sup>[26]</sup> In 2013–2015, the group of Mac-



**Scheme 2.** (a) Reaction of a bromomalonate substrate with indole as radical trap. (b) Perfluoroalkylation of heteroarenes.  $^{19}\text{F}$ -NMR yields (using  $\text{C}_6\text{F}_6$  as internal standard) are provided for the trifluoromethylation products due to volatility of the products, isolated yield reported for **5r**.



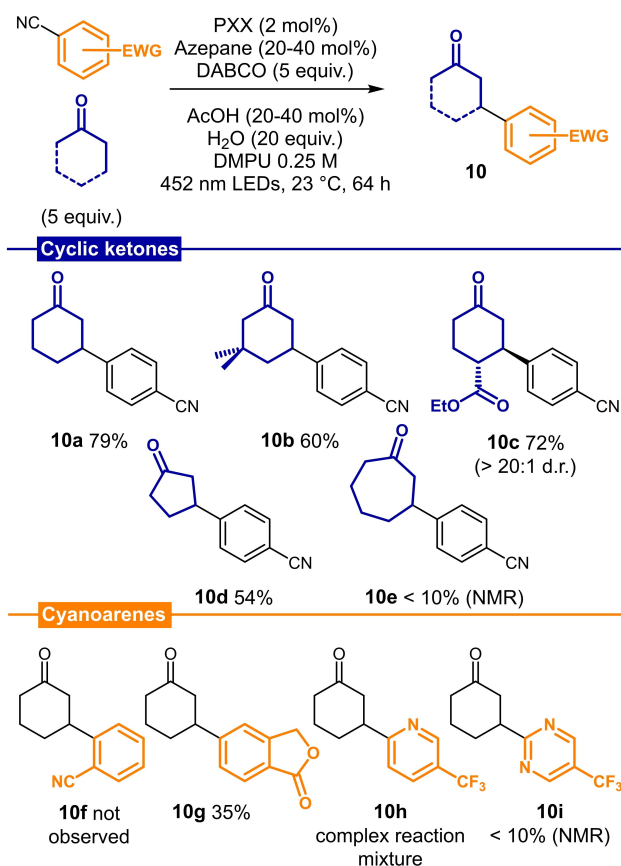
**Scheme 3.** Postulated mechanism for the PXX-photocatalysed addition of aryl radicals to radical traps (in this case, a 5-membered heterocycle).

Millan reported a series of  $\beta$ -functionalisations of saturated carbonyl compounds (aldehydes and cyclic ketones).<sup>[27]</sup> While the  $\alpha$  position of carbonyl deriva-

tives is easily accessible from the formation of enolate or enamine intermediates, limited examples were reported for the  $\beta$  functionalisation without using  $\alpha,\beta$ -unsaturated compounds in the first place. In particular, a  $\beta$ -arylation reaction was carried out with *fac*-[Ir(ppy)<sub>3</sub>] as photocatalyst and electron-deficient benzonitrile derivatives as reactants.<sup>[27a]</sup> When the reaction of cyclohexanone with 1,4-dicyanobenzene was tested in the same conditions using PXX as photocatalyst (Scheme 4),  $\beta$ -arylated product **10a** was obtained in 79% yield.

Applying the reaction conditions to other ketones,  $\beta$ -arylated derivatives could be obtained in 60–72% yields with different cyclohexanone precursors (**10b–c**). Cyclopentanone **10d** was also obtained in 54% yield, while cycloheptanone **10e** could not be recovered in good amounts (less than 10% yield by NMR). When turning to other cyanoarenes, only 4-cyanophthalide afforded **10g** in a modest 35% yield. Other substrates provided limited or no conversion (**10f**, **10i**) or complex reaction mixtures (**10h**).

The mechanism of this transformation was further studied by photophysical and EPR studies. Stern-Volmer fluorescence quenching experiments (Table 3)



**Scheme 4.** Scope of the PXX-catalysed  $\beta$ -arylation of cyclic ketones with cyanoarenes. Isolated yields reported unless otherwise stated.

**Table 3.** Redox potentials and quenching studies on PXX ( $4 \times 10^{-5}$  M in  $\text{CH}_3\text{CN}$ , intensity of fluorescence recorded at 477 nm).

#	Quencher	$E_{\text{red}}$ (V) <sup>[a]</sup>	$k_{\text{Q}}$ ( $\text{M}^{-1}\text{s}^{-1}$ ) <sup>[d]</sup>
1	<b>11a</b>	-1.64 (r)	$1.6 \times 10^{10}$
2	<b>11b</b>	-1.90 (r)	$1.2 \times 10^{10}$
3	<b>11c</b>	-1.59 (r)	$1.6 \times 10^{10}$
4	<b>11d</b>	-1.53 (r)	$1.5 \times 10^{10}$
5	Cyclohexanone	-2.33 (r)	N.D. <sup>[e]</sup>
6	Azepane	$\cong +0.9$ (o) <sup>[b]</sup>	N.D. <sup>[e]</sup>
7	<b>12</b>	+0.3–+0.5 (o) <sup>[c]</sup>	$1.4 \times 10^{10}$
8	DABCO	+0.69 (o)	$2.2 \times 10^8$

<sup>[a]</sup> Determined in  $\text{CH}_3\text{CN}$ ; (r) refers to a reduction of the quencher, (o) to an oxidation of the quencher. Entries 3 and 4: experimentally determined (see SI). Other entries: obtained from reference.<sup>[15]</sup>

<sup>[b]</sup> Typical values for cyclic secondary amines.

<sup>[c]</sup> Typical values for enamines of cyclic secondary amines.

<sup>[d]</sup> Calculated from Stern Volmer plots as  $k_{\text{Q}} = K_{\text{SV}}/\tau_0$  where  $\tau_0$  is the lifetime of PXX\* without quencher (5.1 ns in  $\text{CH}_3\text{CN}$ ).<sup>[14a]</sup>

<sup>[e]</sup> No quenching observed.

revealed that all four electron-poor cyanoarenes examined (entries 1–4) to be efficient quenchers of PXX\*, with quenching constant values in the order of  $10^{10} \text{ M}^{-1} \text{ s}^{-1}$ . This result comes as no surprise, as all their reduction potentials are accessible by PXX\* ( $E^{1/2}(\text{PXX}^{*\cdot+}/\text{PXX}^*) = -2.0 \text{ V vs SCE}$ ). With cyclohexanone (entry 5) and azepane (entry 6) no fluorescence quenching was observed. However, a limited quenching was detected when cyclohexanone, azepane and acetic acid were combined in a single solution. We thus prepared and analysed enamine **12** as quencher (entry 7). Notably, a high quenching constant was obtained ( $1.5 \times 10^{10} \text{ M}^{-1} \text{ s}^{-1}$ ), of the same order of magnitude as that obtained with the cyanoarenes ( $1.2$ – $1.6 \times 10^{10} \text{ M}^{-1} \text{ s}^{-1}$ ). DABCO is also a possible quencher, but with two orders of magnitude lower rate ( $2.2 \times 10^8 \text{ M}^{-1} \text{ s}^{-1}$ , entry 8).

Taken all together, these results suggest both an oxidative photocatalytic mechanism (Scheme 5a, right side), reliant on the photoreduction of cyanoarenes,<sup>[27a]</sup> and a reductive photocatalytic cycle (Scheme 5a, left side), based on the photooxidation of **12** and/or DABCO.<sup>[27d]</sup> In the former mechanism, PXX\* would reduce the cyanoarene to its radical anion **13**, while the resulting PXX<sup>•+</sup> cation ( $E = +0.77 \text{ V vs SCE}$ ) would be capable to oxidise enamine **12** to its radical cation

**14**, reforming PXX. In the latter cycle the parts would be inverted, with PXX\* oxidising enamine **12** to **14**, and the resulting highly reducing PXX<sup>•-</sup> ( $E = -2.16 \text{ V vs SCE}$ ) reducing **11a** to **13**. In either case, the so-formed enamine radical cation **14** would undergo deprotonation by DABCO in the  $\beta$  position to form  $5\pi$ -enaminy radical **15**. Subsequent steps include radical-radical coupling between **15** and **13** to give **16**, loss of a cyanide to give enamine **17** and final hydrolysis to the product (**10a**) while regenerating the organocatalyst.<sup>[27a]</sup>

To further support the mechanistic propositions, EPR measurements were performed to identify the presence of the relevant radicals (Figure 4). The reaction with 1,4-dicyanobenzene **11a** and cyclohexanone yielding product **10a** was performed in the presence of *N*-tert-butyl- $\alpha$ -phenylnitron (PBN) as a radical spin trap.

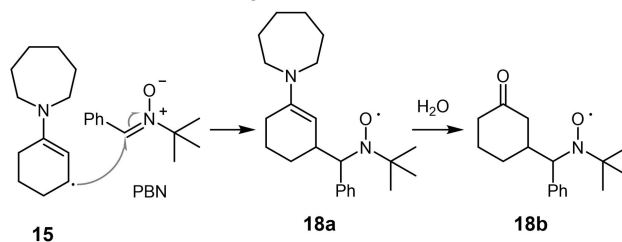
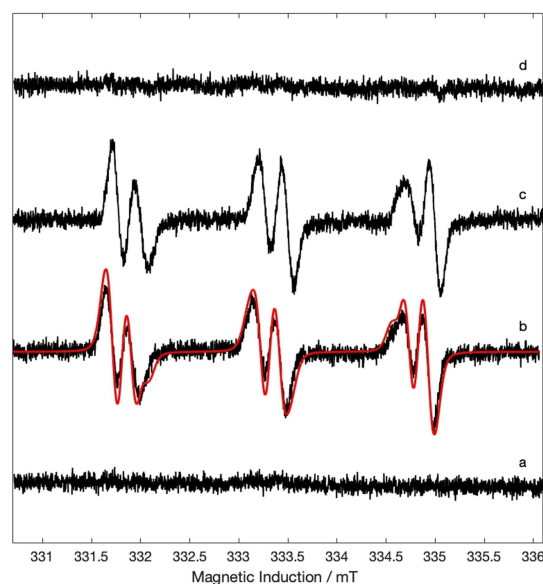
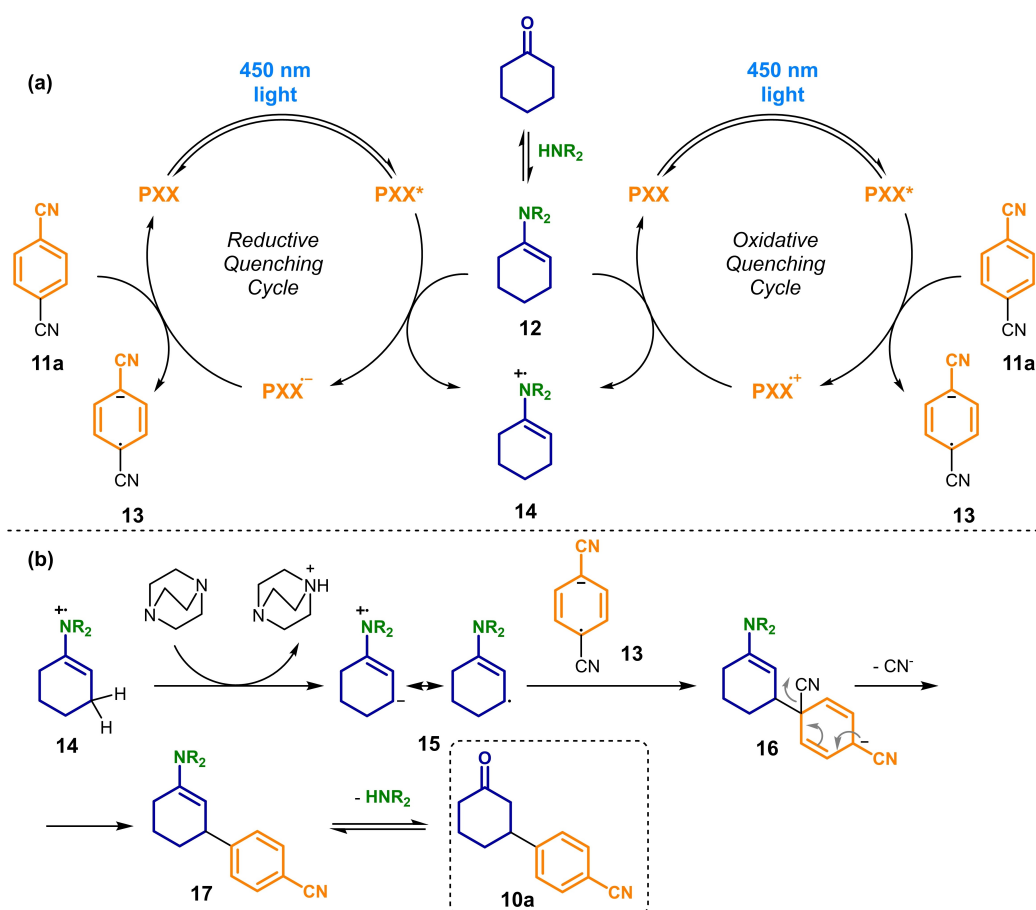


**Figure 4.** Continuous wave EPR spectra of a reaction medium composed of 1,4-dicyanobenzene, cyclohexanone, azepane, PXX, AcOH and  $\text{CH}_3\text{CN}$  with the addition of PBN spin trap measured at rt and (a) before light irradiation, (b) after 30 minutes of irradiation at 450 nm; (c) reaction medium without 1,4-dicyanobenzene after ca. 2 hours of irradiation at 450 nm; (d) reaction medium without cyclohexanone, azepane and acetic acid after 30 minutes of irradiation at 450 nm. Below: structure of PBN-trapped radicals **18a** and **18b**.



**Scheme 5.** Proposed mechanisms for the PXX-photocatalysed  $\beta$ -arylation of cyclic ketones: (a) reductive and oxidative quenching mechanistic cycles; (b) downstream pathway with formation of the product and regeneration of the organocatalyst.

The reaction mixture was measured before and after 30 minutes of irradiation at 450 nm (Figure 4). Whilst before irradiation no detectable EPR signal was observed (Figure 4a), after 30 minutes of irradiation a clear triplet of doublets pattern arose (Figure 4b). Simulation of the signal in Figure 4b highlighted the presence of two PBN-trapped radical species (R1-PBN and R2-PBN), characterized by the following spin Hamiltonian parameters: R1-PBN:  $g_{iso}=2.006$ ,  $a_{iso}(^{14}\text{N})=1.47$  mT,  $a_{iso}(^1\text{H}_\beta)=0.36$  mT (spectral contribution 23 %) and R2-PBN:  $g_{iso}=2.006$ ,  $a_{iso}(^{14}\text{N})=1.51$  mT,  $a_{iso}(^1\text{H}_\beta)=0.18$  mT (spectral contribution 77 %). Cross checks have been performed by removing each of the reaction substrates (*i.e.*, either 1,4-dicyanobenzene or cyclohexanone + azepane) to prove that the trapped radical species observed do indeed come from the reaction and are not byproducts from PBN decomposition under irradiation or other species present in the reaction medium. When 1,4-dicyanobenzene was removed from the reaction medium, another spectrum like that in Figure 4b was detected, with the same trapped radical species (Figure 4c). On the contrary, when cyclohexanone and azepane were

removed from the reaction medium, no paramagnetic species were detected in continuous wave mode (Figure 4d).

This evidence seems to indicate that the PBN-trapped radical species (signals R1- and R2-PBN) both arise from the combination of azepane and cyclohexanone. Given the systematic lack in the literature of comparative examples about PBN-trapped cyclohexanoyl radicals in CH<sub>3</sub>CN, we resort to DFT to assign the signals of radicals R1-PBN and R2-PBN. The structure of 3-cyclohexanoyl PBN adduct **18b** as well as its enamino form **18a**, derived from addition of PBN to 5 $\pi$ -enaminyl radical **15** (Figure 4), were first geometry optimized at the B3LYP/def2-TZVP level of theory (SI). Spin Hamiltonian parameters were calculated on the optimized structures at the PBE0/EPR-II level of theory, *i.e.* a commonly used combination of functional and basis set for the light elements such as H and B-F. These calculations returned the following spin Hamiltonian parameters; PBN-trapped cyclohexanoyl adduct **18b**:  $g_{iso}=2.006$ ,  $a_{iso}(^{14}\text{N})=1.12$  mT,  $a_{iso}(^1\text{H}_\beta)=0.37$  mT; PBN-trapped cyclohexanoyl adduct enamino form **18a**:  $g_{iso}=2.006$ ,  $a_{iso}(^{14}\text{N})=$

1.03 mT,  $a_{iso}(^1H_\beta) = 0.11$  mT. Theoretical  $^1H_\beta$  isotropic hyperfine coupling constants are significantly different between the two optimized structures, and almost completely match the values measured for the two experimental signals, R1-PBN and R2-PBN, of 0.36 mT and 0.18 mT. As to the  $^{14}N$  isotropic hyperfine coupling constants, the theoretical values are generally significantly lower than the experimental values shown by radicals R1-PBN and R2-PBN; however, the difference between the two values is much more contained, *i.e.* 0.09 mT, resembling the 0.04 mT separating the experimental values (on the contrary the  $^1H_\beta$  are much further apart, *i.e.* 0.26 mT for the theoretical values and 0.18 mT for the experimental values). Based on the comparison between theory and experiments, one could assign the R1-PBN signal to the PBN-trapped cyclohexanoyl radical (**18b**) and the R2-PBN signal to the enamino form of the PBN-trapped cyclohexanoyl radical (**18a**), unambiguously providing evidence for the formation of radical **15** in the reaction mixture.

EPR also allowed to ascertain further aspects of the reaction mechanism. Fluorescence quenching studies suggest that both oxidative and reductive mechanisms (Scheme 5a) are possible, and in the case of the reaction with all the components (Figure 4b) both mechanisms fit the EPR results. Considering the high value of the fluorescence quenching constant and the high concentration of the cyanoarenes in solution, the oxidative photocatalytic cycle seems favoured. However, the fact that an almost identical EPR spectrum is obtained in the absence of 1,4-dicyanobenzene (Figure 4c) would suggest that a reductive quenching cycle is in operation. While reduction of cyanoarenes by PXX\* is possible, the fate of the resulting radical ion pair might not include reaction with enamine **12** and eventual delivery of the product, as other processes can occur. For example, upon irradiation cyanoarenes are known to form complexes with electron donor molecules (D) such as pyrenes.<sup>[28]</sup> These complexes are usually in equilibrium with the spin-correlated radical ion pair  $[D^{\bullet+} \cdot \text{cyanoarene}^{\bullet-}]$  following single electron transfer. Back electron transfer (BET) could then occur, with the result of quenching of the radicals, a process that is facilitated by  $CH_3CN$  when used as a solvent.<sup>[28]</sup> A similar behaviour can be postulated for the interaction of cyanoarenes with PXX as an electron donor. Further experiments involving time-resolved EPR and other spin-chemistry techniques, which are beyond the scope of this paper, will be used to quantify kinetic aspects of the interaction of PXX with cyanoarenes. Nonetheless, under our reaction conditions the complete absence of EPR signals when cyclohexanone and azepane are not added to the reaction medium (Figure 4d) seems to suggest that the kinetics involving the dicyanobenzene radical anion, including BET, are much faster than the trapping reaction with PBN and that none of the dicyanoben-

zene radicals live long enough to be seen as a free, not trapped species over the time scales of the continuous wave EPR experiment.

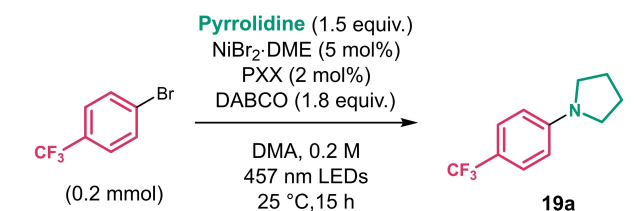
## Nickel-PXX Dual Catalysis: Cross-Coupling Reactions

In recent years, nickel catalysis has seen renewed interest for the possibility to replace catalysts based on more precious metals and the development of new cross-couplings reactions,<sup>[29]</sup> often in combination with photoredox catalytic manifolds.<sup>[30]</sup> Examples include cross-couplings using Ni-photoredox dual catalysis to form C-heteroatom bonds:<sup>[31]</sup> C–N,<sup>[5,32]</sup> C–O,<sup>[33]</sup> C–S<sup>[5a,16,34]</sup> and C–P<sup>[35]</sup>. Considering the chemical stability and low cost of PXX, we envisaged to use it as the photocatalyst partner in the Ni-catalysed cross-coupling reaction to form C-heteroatom bonds. At first, we have explored the reaction of aryl bromides with secondary amines to form C–N bonds. Applying a standard set of conditions<sup>[32a]</sup> with  $NiBr_2 \cdot DME$  as Ni source, DABCO as base and PXX as photocatalyst revealed a very efficient reaction, providing quantitative yields of **19a** in the reaction of pyrrolidine with 4-bromobenzotrifluoride (Table 4).

The reaction was robust as small variations were well tolerated. For example, the PXX loading could be

**Table 4.** Screening of conditions for the PXX-photocatalysed Ni-photoredox cross-coupling of pyrrolidine and 4-bromobenzotrifluoride.

*Standard conditions:*

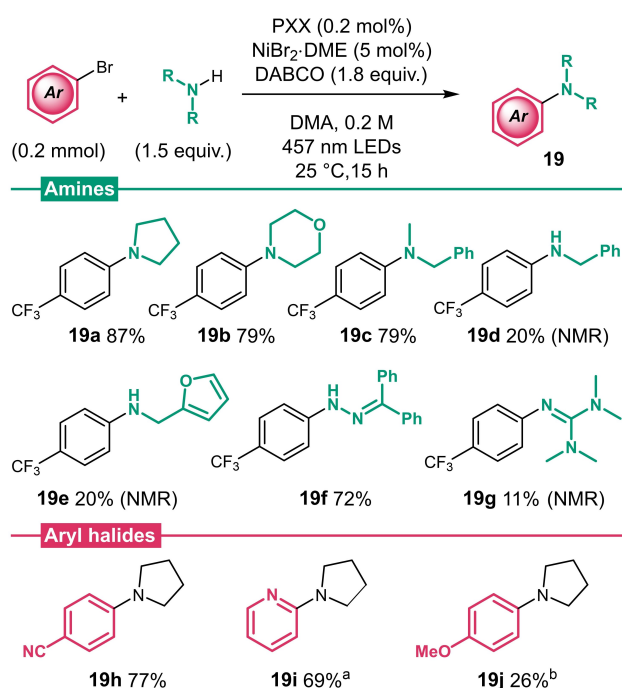


#	Modification	Yield % <sup>[a]</sup>	Conv. % <sup>[a]</sup>
1	4 mol% PXX	97	100
2	none (2 mol% PXX)	94	100
3	1 mol% PXX	99	100
4	0.5 mol% PXX	99	100
5	0.2 mol% PXX	99 (87)	100
6	0.1 mol% PXX	96	100
7	0.2 mol% PXX, 10 mol% Ni	99	100
8	0.2 mol% PXX, 1 mol% Ni	96	97
9	$NiCl_2$ DME as Ni source	95	100
10	DMF as solvent	95	100
11	Acetonitrile as solvent	79	98
12	No PXX	13	13

<sup>[a]</sup> Determined by  $^1H$  NMR analysis of crude products, using 1,3,5-trimethoxybenzene as internal standard. Isolated yield in parentheses.

varied from 2 mol% to 0.1 mol% without losses in efficiency (entries 1–6). Similarly, Ni loading can also be reduced to 1 mol% with only a minor reduction in yield (entry 8). Alternative Ni salts and solvents also provided efficient reactions (entries 9–10) with the exception being CH<sub>3</sub>CN, still giving 79% yield (entry 11). Lastly, in absence of PXX only minor reactivity is observed (13% yield, entry 12), in line with the hypothesis of background photoactivity of the Ni complexes advanced by Miyake and co-workers.<sup>[36]</sup>

The conditions found above were thus applied to a range of aryl halides and amine reaction partners (Scheme 6). Secondary amines efficiently deliver coupled products **19a–c** (79–87% yield), with reactions almost devoid of impurities. Unfortunately, primary amines showed only limited reactivity (**19d–e**, 20% yield by NMR), and every attempt to increase the yield (for example, by heating the reaction mixture to 50 °C) did not provide any improvement. Pleasingly, benzophenone hydrazone is also a competent substrate, and derivative **19f** was obtained in 72% yield. Guanidine **19g** was obtained in limited yields (11%), and also in this case attempts to improve them were not fruitful. Examining other aryl bromides, electron-poor substrates provide products in good yields (**19h–i**, 69–77% yield), while for electron-rich ones the reaction is more difficult, and **19j** was obtained in

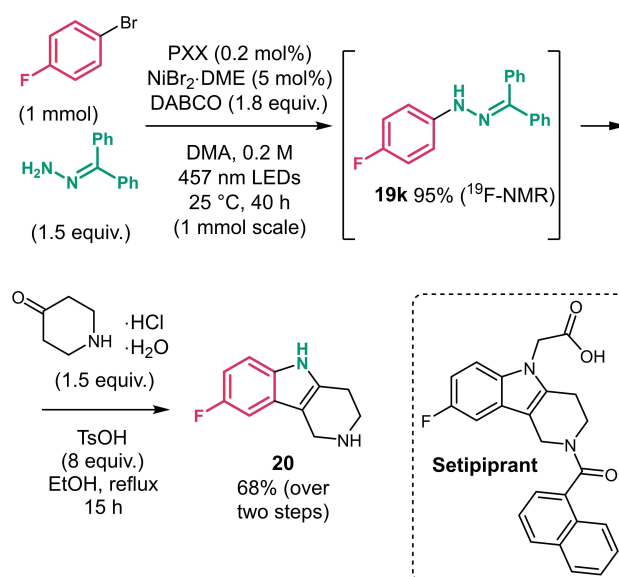


**Scheme 6.** Scope of the Ni-photoredox C–N cross-coupling. Isolated yields are reported, unless otherwise stated. <sup>1</sup>H NMR yields are determined using 1,3,5-trimethoxybenzene as internal standard. Notes: <sup>[a]</sup> Reaction time: 64 h. <sup>[b]</sup> 4-Anisyl iodide used as substrate.

26% yield only by using 4-anisyl iodide in place of the bromide congener.

The good reactivity found with benzophenone hydrazone was particularly intriguing. Products such as **19f** can be regarded as masked hydrazines, important substrates for the formation of indole rings through a Fisher indole synthesis reaction.<sup>[37]</sup> When coupling conditions were applied to 4-bromofluorobenzene and benzophenone hydrazone, *N*-arylhyazone **19k** was obtained with 95% NMR yield (Scheme 7). While **19k** was found to be prone to hydrolysis (both through aqueous washings and column chromatography on silica gel), the reaction mixture after evaporation of the solvent can be directly subjected to Fisher indole synthesis conditions with an enolisable ketone to form fluoro-tetrahydro-1*H*-pyrido[4,3-*b*]indole **20** in 68% yield (over two steps). Indole derivative **20** is a crucial intermediate for the investigational drug setipiprant, under study for treating asthma and scalp hair loss.<sup>[38]</sup> Considering that the reaction was performed on a synthetically useful mmol scale, it demonstrates the possibility to scale this reaction up in a laboratory setting.

The attention was then turned to the C–S bond-forming cross-coupling reaction. Under conditions analogous to those suggested by Oderinde and co-workers,<sup>[16]</sup> the reaction between 4-tolylbromide and octanethiol was found to be difficult (Table 5, entries 1–2). By replacing the former with 4-tolyl iodide the reactivity changed dramatically, and the coupled product **21a** could be obtained quantitatively (entry 3). It was possible to reduce the loading of PXX and Ni pre-catalyst to 0.2 mol% and 5 mol% respectively (entries 4–6). Changing the Ni pre-catalyst or solvent



**Scheme 7.** Application of the Ni-photoredox C–N cross-coupling to **20**, a synthetic intermediate of setipiprant.

**Table 5.** Screening of conditions for the PXX-photocatalysed Ni-photoredox cross-coupling of 4-halotoluenes and octane-thiol.

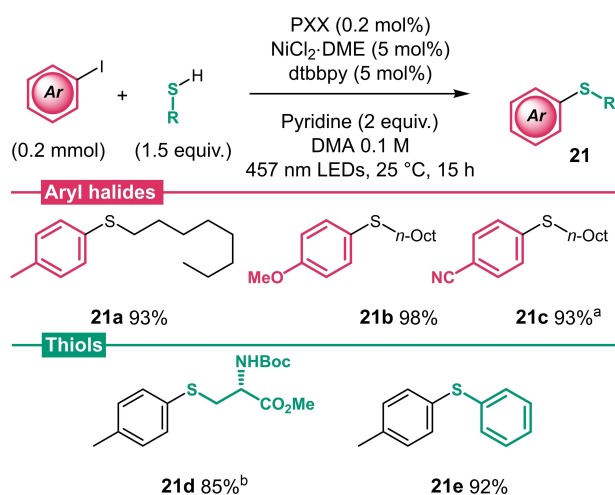
*Standard conditions:*

#	X	Modification	Yield % <sup>[a]</sup>
1	Br	none	23
2	Br	0.2 mol% PXX	0
3	I	none	> 99
4	I	0.4 mol% PXX	> 99
5	I	0.2 mol% PXX	98
6	I	0.2 mol% PXX, 5 mol% Ni/L	> 99 (93)
7	I	NiBr <sub>2</sub> DME as Ni source	99
8	I	DMF as solvent	> 99
9	I	Acetonitrile as solvent	> 99
10	I	No PXX	0

<sup>[a]</sup> Determined by <sup>1</sup>H NMR analysis of crude products, using 1,3,5-trimethoxybenzene as internal standard. Isolated yield in parentheses.

(DMF, or CH<sub>3</sub>CN) did not provide any loss in reactivity (entries 7–9). In the absence of PXX, the reaction does not proceed at all (entry 10).

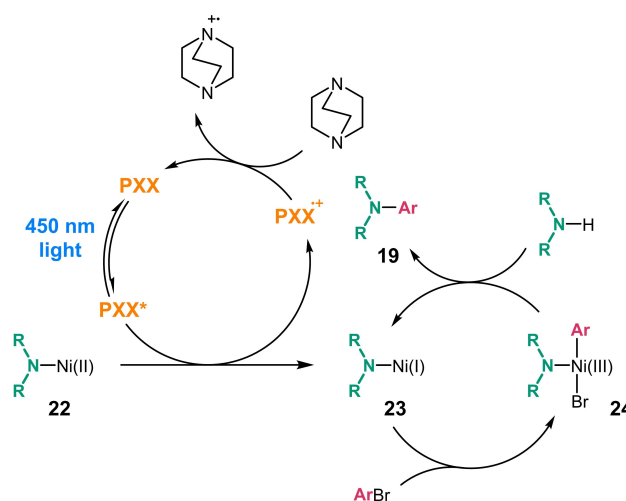
With the conditions found in entry 6, a brief scope of the transformation was examined (Scheme 8). Aryl iodides bearing electron-rich groups worked well (**21 a–b**, 93–98% yield) and in the case of an electron-poor system the aryl bromide could be used as substrate: **12 c** was obtained in 93% yield using 4-bromobenzoni-



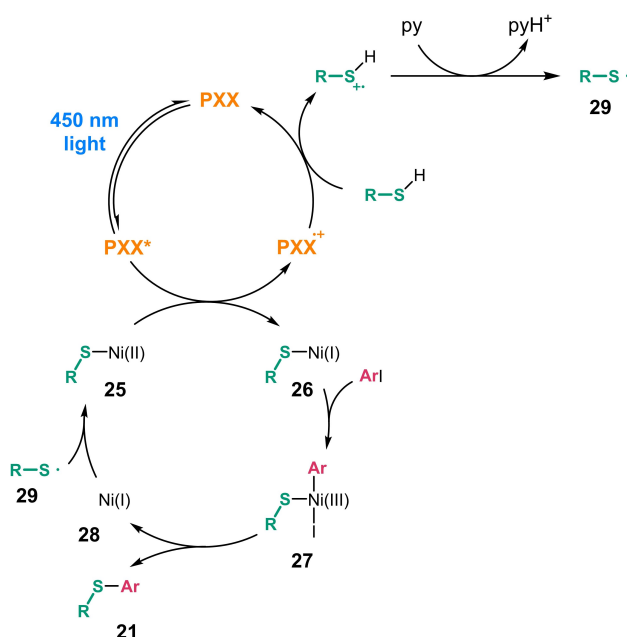
**Scheme 8.** Scope of the Ni-photoredox C–S cross-coupling. Isolated yields are reported. Notes: <sup>[a]</sup> 4-Bromobenzonitrile used as substrate. <sup>[b]</sup> Reaction time: 40 h.

trile. Examining other thiols, a more complex system as found in a protected cysteine is still amenable to reaction: a 85% yield of **21 d** was obtained after 40 h. An aryl thiol in thiophenol is also a viable substrate, and **21 e** was isolated in 92% yield.

The mechanistic understanding of these cross-couplings typically rely on the possibility to control the oxidation state of the Ni centre by the photocatalyst, which would circumvent difficult steps such as the reductive elimination of C-heteroatom bonds from a catalytic Ni(II) complex intermediate.<sup>[16,32a,39]</sup> Further studies have revealed that energy transfer mechanistic manifolds are also possible, extending the range of photocatalysts that can be applied to these transformations as different photophysical properties are relevant depending on the mechanism.<sup>[5b,32c,33b,40]</sup> When considering the C–N cross-coupling, electrochemical considerations make us believe that PXX acts in controlling the oxidation state of the metal. Recent studies from MacMillan and co-workers revealed a Ni(I)/Ni(III) pathway to be operating, where the photocatalyst acts as an initiator by reducing key Ni(II)-amino complexes (resting state) to Ni(I).<sup>[39c]</sup> The high reducing power of PXX\* and PXX<sup>•-</sup> (–2.00 V and –2.16 V, respectively) well matches the requirements found by MacMillan for the iridium photocatalysts ( $E < -1.26$  V vs SCE), whereas the oxidising potentials of PXX\* and PXX<sup>•+</sup> (+0.61 and +0.77, respectively) are high enough to oxidise DABCO, as suggested by our quenching studies and electrochemical considerations (Table 3, entry 8). Taking all this together, we hypothesized the catalytic cycle depicted in Scheme 9. Once the Ni(I) species **23** is formed by reduction of Ni(II) (**22**), oxidative addition of the aryl bromide generates an aryl-Ni(III) species **24** that can undergo reductive elimination to furnish the C–N bond



**Scheme 9.** Postulated mechanism for the PXX- and Ni-catalysed C–N cross-coupling reaction.



**Scheme 10.** Postulated mechanism for the PXX- and Ni-catalysed C–S cross-coupling reaction.

(product **19**). Turnover of the photocatalyst can be achieved by oxidation of DABCO. A similar reductive quenching cycle with initial oxidation of DABCO by PXX\* could also be considered.

PXX might take a similar role in the mechanism of the C–S cross-coupling reaction as well. Building on the studies performed by Oderinde and co-workers,<sup>[16]</sup> we postulate the possibility of reduction of Ni(II) to catalytically-competent Ni(I) by PXX\*. Moreover, oxidation of the thiol is a likely step, which PXX•+ (+0.77 V vs SCE) seems to be able to achieve (e.g., benzylthiol has an oxidation potential of +0.83 V vs SCE in CH<sub>3</sub>CN).<sup>[16]</sup> Based on these considerations, a possible mechanism is depicted in Scheme 10. PXX\* effects the necessary reduction of Ni(II) complexes such as **25** to Ni(I) (**26**), enabling the oxidative addition of the aryl bromide to form an aryl-Ni(III) complex **27**, which undergoes reductive elimination to form the aryl sulfide **21**. Generated PXX•+ oxidises the thiol, forming after deprotonation thiyl radical **29**, which can be intercepted by the Ni(I) centre (**28** to **25**).

## Conclusion

In conclusion, the ability of PXX as photocatalyst to promote a wide variety of radical reactivities was demonstrated, in particular in reactions typical of the more common yet expensive Ir(III) complexes. The relatively high reduction potential of its excited state allows reduction of aryl, alkyl and perfluoroalkyl halides (and chlorides in particular); the resulting organic radicals can then add to suitable radical traps

to form new C–C bonds. Turning the attention to more complex catalytic manifolds, PXX photocatalysis has been successfully coupled with both organocatalysis and metallocatalysis. In the first instance, a  $\beta$ -arylation of cyclic ketones with cyanoarenes was shown to be productive. A range of mechanistic experiments have revealed that a reductive mechanism cycle seems more probable than the normally-accepted oxidative catalytic cycle. It was also possible to identify adducts of the radical trap PBN with potential radical intermediates. Some Ni-catalysed cross-couplings were also promoted by PXX-based photocatalysis, allowing the formation of C–N and C–S bonds from aryl halides and demonstrating effective partnership with metallocatalysis. To the best of our knowledge, this work is one of the few examples of wide demonstrations of reactivity for a new highly reducing organic photocatalyst, thus adding another precious tool to the array of photocatalysts to be chosen for expanding the chemical space of photoredox reactions. Compared to other photocatalysts, PXX stands out for its very low reduction potential of the singlet excited state (–2.0 V vs SCE) coupled to structural simplicity, low cost and ease of preparation (see SI). Further studies are underway to expand the application of PXX-based photocatalysis to the preparation of other classes of compounds.

## Experimental Section

Experimental procedures and characterisation data are reported on the supporting information (PDF). Geometry optimisation data for adduct **18a** (XYZ). Geometry optimisation data for adduct **18b** (XYZ). EPR computational data for adduct **18a** (OUT). EPR computational data for adduct **18b** (OUT).

## Acknowledgements

The authors thank Hugo Morren (Dr. Reddy's) and Tommaso Battisti (Cardiff University) for important analytical support. D.B. and R.D. thank the EU and H2020-MSCA-ITN-2016 (project n° 722591–PHOTOTRAIN) for the generous funding. C.P. and O.M. thank the EU through the PHOTOTRAIN project for a pre-doctoral fellowship. D.B. thanks the University of Vienna for financial support.

## References

- [1] a) J. W. Tucker, C. R. J. Stephenson, *J. Org. Chem.* **2012**, *77*, 1617–1622; b) C. K. Prier, D. A. Rankic, D. W. C. MacMillan, *Chem. Rev.* **2013**, *113*, 5322–5363; c) D. Ravelli, M. Fagnoni, A. Albini, *Chem. Soc. Rev.* **2013**, *42*, 97–113; d) T. Koike, M. Akita, *Inorg. Chem. Front.* **2014**, *1*, 562–576; e) M. H. Shaw, J. Twilton, D. W. C. MacMillan, *J. Org. Chem.* **2016**, *81*, 6898–6926; f) N. A. Romero, D. A. Nicewicz, *Chem. Rev.*

- 2016, *116*, 10075–10166; g) J.-P. Goddard, C. Ollivier, L. Fensterbank, *Acc. Chem. Res.* **2016**, *49*, 1924–1936.
- [2] a) K. A. King, P. J. Spellane, R. J. Watts, *J. Am. Chem. Soc.* **1985**, *107*, 1431–1432; b) J. D. Nguyen, E. M. D. Amato, J. M. R. Narayanam, C. R. J. Stephenson, *Nat. Chem.* **2012**, *4*, 854–859; c) Y. Cheng, X. Gu, P. Li, *Org. Lett.* **2013**, *15*, 2664–2667; d) H. W. Shih, M. N. Vander Wal, R. L. Grange, D. W. C. MacMillan, *J. Am. Chem. Soc.* **2010**, *132*, 13600–13603.
- [3] a) I. Ghosh, L. Marzo, A. Das, R. Shaikh, B. König, *Acc. Chem. Res.* **2016**, *49*, 1566–1577; b) M. Majek, A. J. Von Wangelin, *Acc. Chem. Res.* **2016**, *49*, 2316–2327.
- [4] a) E. H. Discekici, N. J. Treat, S. O. Poelma, K. M. Mattson, Z. M. Hudson, Y. Luo, C. J. Hawker, J. R. De Alaniz, *Chem. Commun.* **2015**, *51*, 11705–11708; b) S. O. Poelma, G. L. Burnett, E. H. Discekici, K. M. Mattson, N. J. Treat, Y. Luo, Z. M. Hudson, S. L. Shankel, P. G. Clark, J. W. Kramer, C. J. Hawker, J. R. De Alaniz, *J. Org. Chem.* **2016**, *81*, 7155–7160; c) M. H. Aukland, M. Šiaučiulis, A. West, G. J. P. Perry, D. J. Procter, *Nat. Catal.* **2020**, *3*, 163–169.
- [5] a) Y. Du, R. M. Pearson, C.-H. Lim, S. M. Sartor, M. D. Ryan, H. Yang, N. H. Damrauer, G. M. Miyake, *Chem. Eur. J.* **2017**, *23*, 10962–10968; b) M. Kudisch, C.-H. Lim, P. Thordarson, G. M. Miyake, *J. Am. Chem. Soc.* **2019**, *141*, 19479–19486.
- [6] L. Wang, J. Byun, R. Li, W. Huang, K. A. I. Zhang, *Adv. Synth. Catal.* **2018**, *360*, 4312–4318.
- [7] R. Matsubara, T. Yabuta, U. Md Idros, M. Hayashi, F. Ema, Y. Kobori, K. Sakata, *J. Org. Chem.* **2018**, *83*, 9381–9390.
- [8] a) I. Ghosh, T. Ghosh, J. I. Bardagi, B. König, *Science* **2014**, *346*, 725–728; b) I. Ghosh, B. König, *Angew. Chem. Int. Ed.* **2016**, *55*, 7676–7679; *Angew. Chem.* **2016**, *128*, 7806–7810; c) J. I. Bardagi, I. Ghosh, M. Schmalzbauer, T. Ghosh, B. König, *Eur. J. Org. Chem.* **2018**, 34–40; d) M. Neumeier, D. Sampedro, M. Májek, V. A. de la Peña O’Shea, A. J. von Wangelin, R. Pérez-Ruiz, *Chem. Eur. J.* **2018**, *24*, 105–108; e) M. Schmalzbauer, I. Ghosh, B. König, *Faraday Discuss.* **2019**, *215*, 364–378; f) N. G. W. Cowper, C. P. Chernowsky, O. P. Williams, Z. K. Wickens, *J. Am. Chem. Soc.* **2020**, *142*, 2093–2099; g) I. A. MacKenzie, L. Wang, N. P. R. Onuska, O. F. Williams, K. Begam, A. M. Moran, B. D. Dunietz, D. A. Nicewicz, *Nature* **2020**, *580*, 76–80; h) A. Graml, T. Nevesely, R. J. Kutta, R. Cibulka, B. König, *Nat. Commun.* **2020**, *11*, Article number: 3174; i) H. Kim, H. Kim, T. H. Lambert, S. Lin, *J. Am. Chem. Soc.* **2020**, *142*, 2087–2092; j) C. Kerzig, X. Guo, O. S. Wenger, *J. Am. Chem. Soc.* **2019**, *141*, 2122–2127.
- [9] I. Ghosh, R. S. Shaikh, B. König, *Angew. Chem. Int. Ed.* **2017**, *56*, 8544–8549; *Angew. Chem.* **2017**, *129*, 8664–8669.
- [10] a) M. Majek, U. Faltermeier, B. Dick, R. Pérez-Ruiz, A. J. von Wangelin, *Chem. Eur. J.* **2015**, *21*, 15496–15501; b) B. D. Ravetz, A. B. Pun, E. M. Churchill, D. N. Congreve, T. Rovis, L. M. Campos, *Nature* **2019**, *565*, 343–346.
- [11] T. Miletić, A. Fermi, I. Orfanos, A. Avramopoulos, F. De Leo, N. Demitri, G. Bergamini, P. Ceroni, M. G. Papadopoulos, S. Couris, D. Bonifazi, *Chem. Eur. J.* **2017**, *23*, 2363–2378.
- [12] a) N. Kobayashi, M. Sasaki, K. Nomoto, *Chem. Mater.* **2009**, *21*, 552–556; b) N. Kobayashi, M. Sasaki, T. Ohe, US Patent 2012/0025173A1, **2012**; c) H. Li, F. Zhang, S. Qiu, N. Lv, Z. Zhao, Q. Li, Z. Cui, *Chem. Commun.* **2013**, *49*, 10492–10494; d) N. Lv, M. Xie, W. Gu, H. Ruan, S. Qiu, C. Zhou, Z. Cui, *Org. Lett.* **2013**, *15*, 2382–2385.
- [13] C. Song, T. M. Swager, *Macromolecules* **2009**, *42*, 1472–1475.
- [14] a) A. Scitutto, A. Fermi, A. Folli, T. Battisti, J. M. Beames, D. M. Murphy, D. Bonifazi, *Chem. Eur. J.* **2018**, *24*, 4382–4389; b) A. Scitutto, A. Berenzin, M. Lo Cicero, T. Miletić, A. Stopin, D. Bonifazi, *J. Org. Chem.* **2018**, *83*, 13787–13798; c) D. Stassen, N. Demitri, D. Bonifazi, *Angew. Chem. Int. Ed.* **2016**, *55*, 5947–5951; *Angew. Chem.* **2016**, *128*, 6051–6055. d) A. Berezin, N. Biot, T. Battisti, D. Bonifazi, *Angew. Chem. Int. Ed.* **2018**, *57*, 8942–8946; *Angew. Chem.* **2018**, *130*, 9080–9084.
- [15] H. G. Roth, N. A. Romero, D. A. Nicewicz, *Synlett* **2016**, 27, 714–723.
- [16] M. S. Oderinde, M. Frenette, D. W. Robbins, B. Aquila, J. W. Johannes, *J. Am. Chem. Soc.* **2016**, *138*, 1760–1763.
- [17] During the preparation of this manuscript, Dilman and co-workers reported the use of PXX as photocatalyst for the iododifluoromethylation of alkenes: A. L. Trifonov, L. I. Panferova, V. V. Levin, V. A. Kokorekin, A. D. Dilman, *Org. Lett.* **2020**, *22*, 2409–2413.
- [18] A. U. Meyer, T. Slanina, C.-J. Yao, B. König, *ACS Catal.* **2016**, *6*, 369–375.
- [19] R. S. Shaikh, S. J. S. Düsel, B. König, *ACS Catal.* **2016**, *6*, 8410–8414.
- [20] a) M. Jiang, H. Yang, H. Fu, *Org. Lett.* **2016**, *18*, 5248–5251; b) A. Nitelet, D. Thevenet, B. Schiavi, C. Hardouin, J. Fournier, R. Tamion, X. Pannecoucke, P. Jubault, T. Poisson, *Chem. Eur. J.* **2019**, *25*, 3262–3266.
- [21] E. C. Swift, T. M. Williams, C. R. J. Stephenson, *Synlett* **2016**, 27, 754–758.
- [22] D. A. Nagib, D. W. C. MacMillan, *Nature* **2011**, *480*, 224–228.
- [23] S. P. Pitre, C. D. McTiernan, J. C. Scaiano, *Acc. Chem. Res.* **2016**, *49*, 1320–1330.
- [24] D. E. Bartak, K. J. Houser, B. C. Rudy, M. D. Hawley, *J. Am. Chem. Soc.* **1972**, *94*, 7526–7530.
- [25] D. A. Nicewicz, D. W. C. MacMillan, *Science* **2008**, *322*, 77–80.
- [26] M. Silvi, P. Melchiorre, *Nature* **2018**, *554*, 41–49.
- [27] a) M. T. Pirnot, D. A. Rankic, D. B. C. Martin, D. W. C. MacMillan, *Science* **2013**, *339*, 1593–1596; b) F. R. Petronijevic, M. Nappi, D. W. C. MacMillan, *J. Am. Chem. Soc.* **2013**, *135*, 18323; c) J. A. Terrett, M. D. Clift, D. W. C. MacMillan, *J. Am. Chem. Soc.* **2014**, *136*,

- 6858–6861; d) J. L. Jeffrey, F. R. Petronijevic, D. W. C. MacMillan, *J. Am. Chem. Soc.* **2015**, *137*, 8404–8407.
- [28] S. Narra, Y. Nishimura, H. A. Witek, S. Shigeto, *ChemPhysChem* **2014**, *15*, 2945–2950 and references cited therein.
- [29] C. C. C. Johansson Seechurn, M. O. Kitching, T. J. Colacot, V. Snieckus, *Angew. Chem. Int. Ed.* **2012**, *51*, 5062–5085; *Angew. Chem.* **2012**, *124*, 5150–5174.
- [30] a) J. Twilton, C. C. Le, P. Zhang, M. H. Shaw, R. W. Evans, D. W. C. Macmillan, *Nat. Rev.* **2017**, *1*, Article number: 0052; b) L. N. Cavalcanti, G. A. Molander, *Top. Curr. Chem.* **2016**, *374*, 39.
- [31] C. Cavedon, P. H. Seeberger, B. Pieber, *Eur. J. Org. Chem.* **2020**, 1379–1392.
- [32] a) E. B. Corcoran, M. T. Pirnot, S. Lin, S. D. Dreher, D. A. DiRocco, I. W. Davies, S. L. Buchwald, D. W. C. Macmillan, *Science* **2016**, *353*, 279–283; b) M. S. Oderinde, N. H. Jones, A. Juneau, M. Frenette, B. Aquila, S. Tentarelli, D. W. Robbins, J. W. Johannes, *Angew. Chem. Int. Ed.* **2016**, *55*, 13219–13223; *Angew. Chem.* **2016**, *128*, 13413–13417; c) T. Kim, S. McCarver, C. Lee, D. W. C. MacMillan, *Angew. Chem. Int. Ed.* **2018**, *57*, 3488–3492; *Angew. Chem.* **2018**, *130*, 3546–3550.
- [33] a) J. A. Terrett, J. D. Cuthbertson, V. W. Shurtleff, D. W. C. Macmillan, *Nature* **2015**, *524*, 330–334; b) E. R. Welin, C. Le, D. M. Arias-Rotondo, J. K. McCusker, D. W. C. MacMillan, *Science* **2017**, *355*, 380–385.
- [34] M. Jouffroy, C. B. Kelly, G. A. Molander, *Org. Lett.* **2016**, *18*, 876–879.
- [35] J. Xuan, T. T. Zeng, J. R. Chen, L. Q. Lu, W. J. Xiao, *Chem. Eur. J.* **2015**, *21*, 4962–4965.
- [36] C. H. Lim, M. Kudisch, B. Liu, G. M. Miyake, *J. Am. Chem. Soc.* **2018**, *140*, 7667–7673.
- [37] S. Wagaw, B. H. Yang, S. L. Buchwald, *J. Am. Chem. Soc.* **1998**, *120*, 6621–6622.
- [38] H. Fretz, A. Valdenaire, J. Pothier, K. Hilpert, C. Gnerre, O. Peter, X. Leroy, M. A. Riederer, *J. Med. Chem.* **2013**, *56*, 4899–4911.
- [39] a) Z.-H. Qi, J. Ma, *ACS Catal.* **2018**, *8*, 1456–1463; b) R. Sun, Y. Qin, S. Ruccolo, C. Schnedermann, C. Costentin, D. G. Nocera, *J. Am. Chem. Soc.* **2019**, *141*, 89–93; c) N. A. Till, L. Tian, G. D. Scholes, D. W. C. MacMillan, *J. Am. Chem. Soc.* **2020**, *142*, 15830–15841.
- [40] a) L. Tian, N. A. Till, B. Kudisch, D. W. C. MacMillan, G. D. Scholes, *J. Am. Chem. Soc.* **2020**, *142*, 4555–4559; b) P. Ma, S. Wang, H. Chen, *ACS Catal.* **2020**, *10*, 1–6; c) J. Lu, B. Pattengale, Q. Liu, S. Yang, W. Shi, S. Li, J. Huang, J. Zhang, *J. Am. Chem. Soc.* **2018**, *140*, 13719–13725.

*peri*-Xanthenoxanthene (PXX): a Versatile Organic Photocatalyst in Organic Synthesis

*Adv. Synth. Catal.* **2021**, *363*, 1–15

 C. Pezzetta, A. Folli, O. Matuszewska, D. Murphy, R. W. M. Davidson\*, D. Bonifazi\*

